Direct Observation of Polymerization-Reaction-Induced Molecular Self-Assembling Process: In-Situ and Real-Time SANS Measurements during Living Anionic Polymerization of Polyisoprene-*block*-polystyrene

Kazuhiro Yamauchi,[†] Hirokazu Hasegawa,[†] Takeji Hashimoto,*[,†,‡,§] Hirokazu Tanaka,[†,‡] Ryuhei Motokawa,[‡] and Satoshi Koizumi[‡]

Advanced Science Research Center, Japan Atomic Energy Agency, Tokai-mura, Ibaraki-ken 319-1195, Japan, and Department of Polymer Chemistry, Graduate School of Engineering, Kyoto University, Katsura, Kyoto 615-8510, Japan

Received December 17, 2005; Revised Manuscript Received March 31, 2006

ABSTRACT: We investigated a simultaneous living anionic polymerization process of isoprene (I) and styrene-d_8 (S) in benzene-d_6 as a solvent with *sec*-buthyllithium as an initiator into polyisoprene(PI)-*block*-poly(styrene-d_8) (PS) and the polymerization-induced molecular self-assembling process. This process was observed in-situ by time-resolved small-angle neutron scattering (SANS) experiment. The SANS profiles measured exhibited three time regions, defined by regions 1−3, with increasing time *t*. In region 1, the SANS profiles exhibited no scattering maxima, and only the intensity level at low scattering vectors *q* increased with time, suggesting the growth of PI chains. In region 2, a scattering maximum appeared at $q = q_m \cong 0.2$ nm^{-1}, the maximum intensity I_m gradually and slightly increased, but q_m hardly changed with *t*, suggesting a gradual change in the living chain ends from isoprenyllithium to styryllithium and formation of PI-*block*-poly(I/S)$^-$ or PI-*block*-polyS$^-$, where poly-(I/S)$^-$ is seemingly a short tapered block chains of I and S monomeric units and polyS$^-$ is a short sequence of S: At the end of region 2, all the chains ends are expected to be the styryllithium. In region 3, q_m and I_m rapidly decreased and increased, respectively, suggesting the growth of PS block chains from the ends of PI-*block*-poly-(I/S)$^-$ or PI-*block*-polyS$^-$: polymerization-induced disorder−order transition and order−order transition were also observed in-situ in this time region. The time-resolved SANS studies enabled us to explore time evolution of hierarchical structures induced by time evolution of the primary structure. Existence of the three time regions seems to reflect different states in ionic association of living chain ends which may be intimately related to the intrinsic kinetics of the copolymerization. It is striking for us to find that k_{SS} in region 2 is very small compared with that in region 3, where k_{SS} is reaction rate constant of S living end to S monomer.

I. Introduction

"Bottom-up"-type nanomaterials, which have been recently spotlighted in many fields, are basically created by building up a large number of molecules one after another into nanostructures according to various self-assembling mechanisms existing in nature. Such molecular self-assembling is sometimes achieved for molecular systems having a sequential connection of a few kinds of simple units. Actually, connecting simple units one after another into a linear sequence creates many functional substances, not only in terms of nanomaterials but also in terms of living organisms. Such systems themselves self-assemble into molecular assemblies having higher-order structures. For instance, proteins are composed of linear sequences of less than 20 kinds of amino acids and bring a miraculous function to life. DNA is also composed of just four kinds of bases (A: adenine; G: guanine; C: cytosine; T: thymine) in linear sequences.

AB diblock copolymer is also considered as a special linear sequence of two simple monomeric units of A and B; a sequence of A is linked to a sequence of B. This special sequence forms a periodical nanopattern called "microdomain structure" with a long-range order, if the segregation power between the two sequences is large enough. This higher-order structure may bring miraculous function as bottom-up type nanomaterials, such as photonic crystals[1] and high-density information-storage media.[2−5]

In this study, we shall investigate the "reaction-induced self-assembling process" of an AB diblock copolymer during living anionic polymerization process as a general problem in the interface between chemistry (reaction at specific sites) and physics (reaction-induced self-assembly at specific sites). Up to now, living anionically synthesized block copolymers (bcp's), which are reaction-terminated and hence "dead" in a sense, have been used to study their self-assembling behaviors. In this case, the total degree of polymerization (DP), *N*, and composition *f* (= N_A/N, N_A being DP of A block sequence) values are fixed during the course of the experiment. However, what would happen if we use a "living" polymer system instead of the reaction-terminated polymer? We can change χ, *N*, and *f* with the progress of the polymerization reaction. Here χ is net repulsive interactions between two block chains in the reaction medium. Controls of reactions in the living polymer system may allow finer controls of the domain structure than the conventional methods.

If χN exceeds the critical value during the polymerization as a consequence of an increase in both the molecular weight of the polymer and the polymer concentration in solution, microphase separation will occur during the polymerization. Let us call this "polymerization-induced microphase transition", since microphase transition is usually induced by changing temperature, pressure, or concentration of the reaction-

* Corresponding author: Tel +81-29-284-3833; Fax +81-29-282-5939; e-mail hashimoto.takeji@jaea.go.jp.
[†] Kyoto University.
[‡] Japan Atomic Energy Agency.
[§] Present address: Advanced Science Research Center, Japan Atomic Energy Agency, Tokai-mura, Ibaraki-ken 319-1195, Japan.

10.1021/ma052696s CCC: $33.50
Published on Web 05/23/2006

terminated bcps. This process of building up a molecule is considered as a kind of the bottom-up process of the self-assembly.

Polymerization-induced microphase transition is quite interesting in terms of morphology control. For instance, when the microphase separation occurs during the polymerization, the living ends of bcps are confined in one side of the microphases (A or B microdomains in the case of AB di-bcp). A further polymerization after the microphase separation occurs in the specific sites of so-called confined nanospace (microdomain structure). As a example, let us consider the case where polymerization of AB di-bcp has completed, and the living ends still exist in the cylindrical microphase rich in B of AB di-bcp. If a further polymerization of C monomer occurs in the B cylindrical microdomains by adding C monomer (in this case, ABC triblock terpolymer is produced), new C microdomains embedded in B cylinders may appear in the A matrix phase. The morphology created here may be generally considered as a nonequilibrium, metastable one and hence may not be necessarily the same as that expected for the corresponding synthesized (and reaction-terminated) ABC triblock terpolymer formed from disordered state. Thus, there is a large possibility to create a new microdomain structure by utilizing polymerization-induced microphase transition. Moreover, if we can directly observe this self-assembling process, we will be able to stop polymerization at the stage when a desired morphology is attained. Thus, direct observation of self-assembling process may bring a breakthrough for manipulation of morphology.

Needless to say, in the reaction-induced self-assembly we are interested in controlling nonequilibrium, metastable morphologies. For achieving the first step of our research along this line, we designed the synthesis of a bcp having high molecular weight in a high concentration solution so that microphase separation takes place during the polymerization reaction. Although there were a number of studies about the self-assembling process of bcp via order−disorder transition (ODT) and order−order transition (OOT) induced by temperature,[6−14] the polymerization-induced ODT and OOT of bcps and its consequence on the self-assembly have never been observed and reported yet.

We adopted the methodology to synthesize AB di-bcp as follows: Polymerization is started in a condition of two monomers coexisting in the solvent without stirring. The large difference in the reactivity between two kinds of monomers guides the polymerization reaction to produce a di-bcp. Since we avoided artificial operations such as stirring, the structural changes during the polymerization process are induced only by self-assembling of the growing molecules themselves.

So far time-resolved SANS has been used as a powerful technique to study dynamics of physical processes in polymer systems such as ODT of bcps[13,14] and shear-induced phase transition of polymer blends.[15,16] However, SANS must be also extremely useful to study chemical reactions in polymer systems such as polymerization,[17−23] gelation,[24−26] etc., because of low energy, high transmittance of neutron beam. The low quantum energy of neutrons is extremely important to avoid artifacts caused by radiation-induced side reactions in reaction systems. In the time-resolved SANS measurement, we must look at not only the chemical reactions process but also structural changes (primary, secondary, and higher-order structures) with increasing the degree of polymerization.

In this paper, we would like to report the preliminary results of our time-resolved SANS study of the living anionic polymerization process of polyisoprene-*block*-poly(styrene-d_8) (PI-*block*-dPS) in benzene-d_6 as a solvent. Since SANS contrast depends on the scattering length density of substances, only nondeuterated isoprene units (I) are highlighted in this system because hydrogen atoms have negative scattering length, while deuterium atoms have positive scattering length. In a nonpolar solvent such as benzene, it is well-known that the anionic reactivity of I is much larger than that of styrene (S). Therefore, we can observe not only the growth of nondeuterated I but also the reaction of deuterated S after consumption of I by means of SANS. This is the first report of our studies on the in-situ observation of self-assembling process induced by a living anionic polymerization.

Table 1. Characteristics of PS-*block*-PI Diblock Copolymer

	$M_n \times 10^{-5}$	M_w/M_n	composition[a]
PS-*block*-PI	1.41	1.03	1:1

[a] The weight ratio of PS:PI.

II. Experiments

The living anionic polymerization was carried out under a dry argon atmosphere in a baked glass tube as a reaction vessel equipped with a three-way stopcock and a magnetic stirring bar. All reagents were transferred into the vessel via dried syringes through the three-way stopcock against a dry argon stream. The synthesis procedure in this study was as follows: A mixture of I, S-d_8, and benzene-d_6 in the ratio of 1:1:2 by weight was introduced into the vessel under a dry argon atmosphere at room temperature. A measured amount of cyclohexane solution of *sec*-butyllithium was added to the mixture via the syringe technique, which gave a light yellow color of isoprenyl anion. In a nonpolar solvent, it is well-known that the anionic reactivity of I is much larger than that of S, resulting in the formation of PI-*block*-dPS bcp even when the two monomers coexist.

As soon as *sec*-butyllithium was added to the mixture, a part of the mixture solution was extracted and introduced into a quartz cell for SANS measurement under a dry argon atmosphere. Immediately, time-resolved SANS measurement was started with the SANS-J instrument installed at 20 MW JRR-3 research reactor at JAEA, Tokai, Japan. Cold neutrons were monochromatized with a velocity selector to have the mean wavelength λ of 0.70 nm and $\Delta\lambda/\lambda = 0.12$. The solution under living anionic reaction in the quartz cell was kept at 30 °C without stirring during time-resolved SANS measurements.

The resulting bcp was characterized by gel permeation chromatography (GPC). The number-average molecular weight M_n and polydispersity index M_w/M_n were estimated from GPC on the basis of polystyrene calibration. Characteristics data of PI-*block*-dPS synthesized in this study are shown in Table 1. The results suggest that a well-controlled polymerization was attained with our method.

III. Results

Figure 1 shows the change in the SANS profiles with reaction time during the living anionic polymerization of I/S-d_8 mixture in benzene-d_6. Scattering intensity is plotted in logarithmic scale against magnitude of scattering vector q ($q = (4\pi/\lambda)\sin(\theta/2)$, where λ and θ are the wavelength of neutrons and the scattering angle, respectively). The counting time for the measured profile during polymerization was varied according to the rate at which the scattering intensity level changes: 5 min from 0 to 29 499 s after the onset of the polymerization, 1 min from 29 851 to 35 457 s, 5 min from 35 544 to 38 719 s, 30 min from 41 512 to 68 044 s. The time shown in the figure legend indicates the onset time for the counting in unit of second for each datum acquisition. The scattering intensity data were corrected for empty cell scattering and sample transmission as well as for the incoherent scattering intensity by subtracting the incoherent

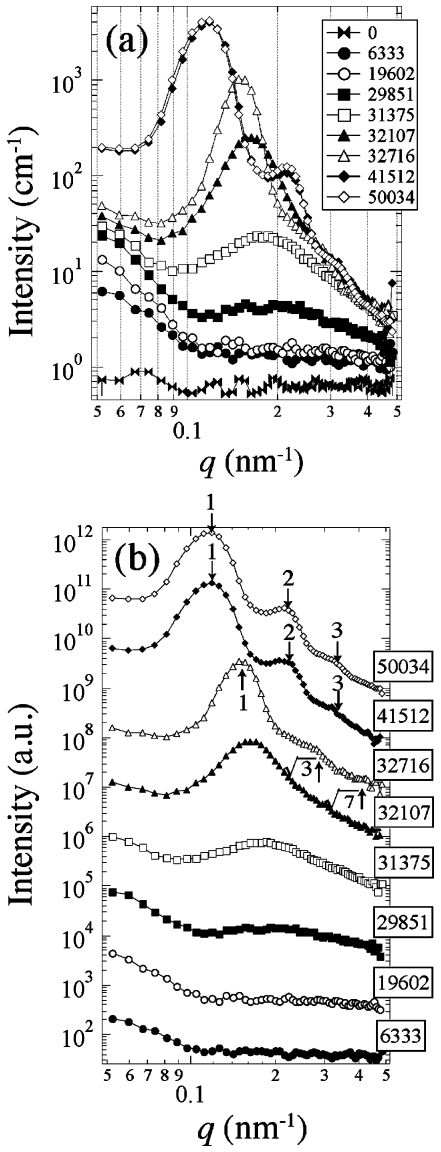

Figure 1. (a) Time dependence of the SANS profiles during the living anionic polymerization of isoprene/styrene-d_8 mixture in benzene-d_6. The intensity is shown in logarithmic scale. The numbers attached to the markers denote the reaction time in seconds. (b) The same data as in (a), but the profiles are shifted vertically for clarity.

scattering intensity from the net observed scattering intensity. The incoherent scattering was estimated from the measured value for I, calculated values for S-d_8 and benzene-d_6, and the respective volume fractions. The corrected intensity was reduced to absolute intensity by calibrating with a secondary standard of an aluminum plate.

The scattering profiles in Figure 1a,b were obtained at t = 6333, 19 602, 29 851, 31 375, 32 107, 32 716, 41 512, and 50 034 s after injection of the initiator; the initiation of polymerization was set at t = 0 s. Figure 1a includes the scattering profile before polymerization (t = 0) also. The profiles in Figure 1b were vertically shifted deliberately to avoid overlapping. In Figure 1a the scattering intensity before polymerization is weak and independent of q. The intensity level at $q > 0.1$ nm^{-1} increases after polymerization. At t = 6333 s, an upturn in the scattering intensity with decreasing q at low q region ($q < 0.1$ nm^{-1}) was observed, although it is not observed before polymerization. The upturn was also observed at t = 19 602 to 33 021 s, though the profile at 33 021 s was not included in the figure.

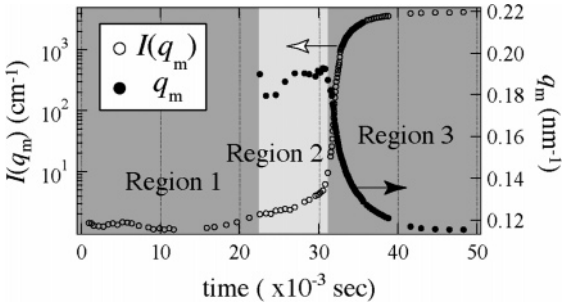

Figure 2. Time evolution of the q_m and the intensity $I(q_m)$ of scattering maximum at $q = q_m = 0.2$ nm^{-1} from t = 300 s to t = 50 034 s. $I(q_m)$: unfilled circles; q_m: filled circles. This polymerization process viewed from SANS was divided into three regions (regions 1−3).

At t = 29 851 and 31 375 s, a scattering peak arising from the correlation hole effect[6,28] was observed in the region of $q \sim 0.2$ nm^{-1}, corresponding to characteristic length of 30 nm. Though the scattering intensity at the peak position $I(q_m)$ increased with time, the peak position (q_m) remained nearly constant. At t = 32 107 s, $I(q_m)$ increased and q_m shifted toward smaller q compared with the profile at t = 31 375 s. At $t >$ 32 716 s, we observed not only an increase in $I(q_m)$ and a decrease in q_m but also the second-order and the third-order scattering peaks. These changes in the scattering profiles shown in Figure 1 suggest that the primary structure of the polymer chains and their higher-order structure dramatically changed during the polymerization process.

Figure 2 shows the time evolution of $I(q_m)$ and q_m from the beginning to the end of polymerization. From the viewpoint of time dependences of the scattering in Figure 2, the polymerization process can be divided into three regions as follows: In region 1, from $t \sim 0$ to 2.25×10^4 s, the upturn in the scattering intensity was observed at low $q < 0.1$ nm^{-1}, and its scattering intensity increased with time. However, the scattering intensity at $q = q_m \cong 0.2$ where the scattering maximum appears at later times only slightly increase with time. In region 2, from $t \sim 2.25 \times 10^4$ to 3.09×10^4 s, a peak appeared at $q = q_m \cong 0.2$ nm^{-1} and $I(q_m)$ gradually and slightly increased with time, while q_m remained almost constant. In region 3, from $t \sim 3.09 \times 10^4$ to the end of polymerization, q_m rapidly shifted toward smaller q, and $I(q_m)$ also rapidly increased; then, higher-order scattering maxima appeared. The details of region 1 to region 3 are discussed below.

IV. Discussion

A. Region 1. The polymer solution had a light yellow color throughout region 1. This color suggests the presence of polyisoprenyllithium (PILi) but not polystyryllithium (PSLi); i.e., the difference in the reactivity of the two monomers in benzene allowed the dominance of PILi despite the coexistence of I and S in the solution. Therefore, region 1 is the period where the *sec*-butyllithium initiator selectively reacts with I, and PILi propagates to increase its chain length. This is consistent with the established law on copolymerization kinetics in nonpolar solvents:[27]

$$k_{SI} > k_{SS} > k_{II} > k_{IS} \quad (1)$$

where k_{JL} is the reaction rate constant for Jth living end to Lth monomer, J and L being either I or S. Since $k_{II} > k_{IS}$, the growing chain ends are dominant in PILi. Even when the chain end happens to react with S to form PSLi, it is rapidly transformed into PILi because $k_{SI} > k_{SS}$.

Since the scattering contrast for SANS exists between PI and the others in the solution (I, S-d_8, and benzene-d_6), and the scattering from thermal concentration fluctuations of I against S-d_8 and benzene-d_6 is negligible compared with the scattering from thermal concentration fluctuations of PILi against others, it is possible to observe only PILi under propagation by means of SANS. The propagation of polyisoprene chains proceeded slowly in our experimental conditions, i.e., without stirring at room temperature. Therefore, enough counting time for SANS measurement was available to follow the polymerization process.

According to a close observation of the SANS profiles in region 1, the intensity upturn at low-q region suggests the existence of large aggregates of PILi in the solution. We expect the large aggregates are comprised of multiplets of ion pairs as proposed by Stellbrink et al.[18] It is crucial to note that PILi did not exist as single chains isolated in the benzene solution but rather aggregated together at the living chain ends to form a fundamental structure unit of star-like structure (multiple-ion pairs) which are further aggregated into the larger aggregates, as proposed by Stellbrink et al.[18] There have been some reports on the aggregation of carbanyllithium polymer at its chain ends in nonpolar hydrocarbon solvents such as cyclohexane and benzene (slightly polar);[17−20] e.g., Fetters et al. also observed an upturn in the SANS intensity at low-q region for polybutadienyllithium in benzene solution and concluded that the living polymers existed as aggregates after the careful analysis.[17] Some old studies proposed such mechanisms that four PILi chain ends should associate together to form a tetramer in hydrocarbon solution,[29−32] and dissociation might occur from tetrameric PILi to dimeric associates with increasing the molar mass of the polymer.[33] In this work we focused on SANS in a small-q region in order to explore the reaction-induced self-assembly of bcp via ODT and OOT. Thus, our data lack the scattering profiles at a larger q region which are required to determine the association number of living chain ends.[17−20] Detailed analysis of the aggregated structure including the association number for this system, however, deserves future work.[21] Hereafter, whenever we refer to aggregates or association, we always refer to the aggregates or association at the living chain ends.

The upturn was not observed before polymerization without initiator (as shown by the profile at $t = 0$ in Figure 1a). Moreover, the upturn disappeared when the living polymerization was terminated by methanol. These results suggest that an association of living anions and their counterions is responsible for the upturn. The weak scattered intensity level of the system before polymerization is due to thermal concentration fluctuations and the contrast difference of I against S-d_8 and benzene-d_6. Since the thermal correlation length is very small, the scattering intensity is independent of q in the observed q range. The intensity level at $q > 0.1$ nm^{-1} and at $t = 6333$ and 19 602 s becomes much higher than that before polymerization due to increase of molecular weight of PI.

In region 1, it is surprising at first sight to note that the scattered intensity at a fixed q value (equal to $q = 0.2$ nm^{-1}, defined as q_m), where the scattering peak appeared in region 2 does hardly change with time as shown in Figure 2. This may be due to a counterbalance of the following two physical factors: (i) the intensity tends to increase with time upon increasing molecular weight of PI with time, but (ii) the intensity tends to decrease with decreasing osmotic compressibility due to increasing polymer concentration with time. We can estimate the time t^* and molecular weight $M(t^*)$ or DP, $N(t^*)$, of PI when the growing PI chains attain the overlap concentration,[28] c^*, as follows. First, we can estimate degree of polymerization, $N(t)$, as a function of time t with the aid of data shown in Figure 3 later. Thus, we can evaluate $c^*(t)$ as a function of t. Second, we can estimate the effective number of growing polymer chains, n_p, per unit volume of the solution from DP of PI chain, N_{PI}, attained at the end of PI polymerization. On the basis of the assumption of an ideal living polymerization such that n_p is constant with t and monomer conversion is 100%, we can estimate concentration of PI chains, $c(t)$, as a function of t. Hence, $N(t^*)$ or $M(t^*)$ can be evaluated from the relationship given by $c(t) = c^*(t)$ at $t = t^*$. From the value $M(t^*)$ and the data in Figure 3 we can evaluate t^*. The evaluation yielded $t^* \cong 4 \times 10^3$ s and $M_n^* = 1.9 \times 10^4$.[34] Actually, PI chains are expanded due to excluded-volume effects so that the systems reach the overlap concentration at an earlier time than this time as estimated above. In conclusion, the overlap concentration is attained at a relatively earlier time in region 1. Thus, it is reasonable to observe the intensity at $q \cong 0.2$ nm^{-1} hardly changes with time in region 1 despite the increase of $M(t)$ with t. After attaining the overlap concentration, the intensity should decrease with t. The experimental fact that the intensity hardly changes with time may infer existence of a counterbalancing effect such that the intensity tends to increase due to an increasing contribution of the large aggregates causing the low-q upturn.

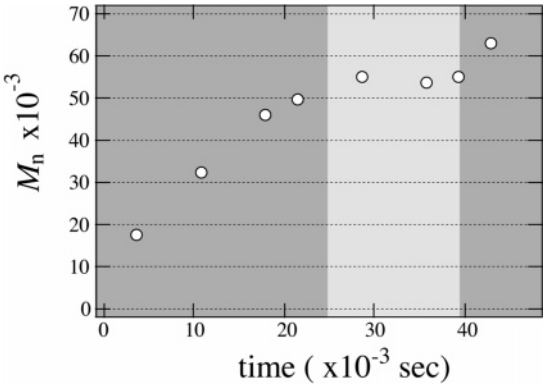

Figure 3. Time dependence of the molecular weight (M_n) during the polymerization.

B. Region 2. In region 2, the scattering peak appeared, indicating formation of the bcp due to addition of styrene-d_8 to the living ends of PILi. The scattering maximum originates from the correlation hole effect[6,28] due to the bcp formation. Actually, the color of the living polymer solution gradually changed in this region from light yellow to red, implying a gradual change in the living chain end from PILi in the end of region 1 to PSLi in the end of region 2. Interestingly enough, the color of the polymer solution did not completely change into red inherent to PSLi until the end of region 2. The chain length of the newly formed block is expected not to increase significantly in region 2, judging from almost constant value of q_m with time.

Figure 3 shows the time dependence of the molecular weight during the polymerization. We carried out another polymerization experiment for the data shown in Figure 3 because we could not extract precursory polymer solutions and measure the molecular weight during the SANS experiment in this preliminary work. However, the experiment to obtain the results shown in Figure 3 was carried out under the same condition as that in the SANS measurement. Therefore, we can directly compare the time dependence of both experiments at least for qualitative discussion. Again, the polymerization process can be divided into three distinct regions as indicated by the darkness of the shaded area in Figure 3.

Table 2. Characteristics of Region 2 and Region 3

region properties	region 2	region 3
solution color	extremely slow change from light yellow to red	red
M_n	nearly constant with time	rapid increase
q_m	nearly constant with time	rapid decrease

In the beginning of the polymerization as shown by the left darkly shaded area in Figure 3, the molecular weight (M_n equivalent to PS standards) of the polymer increased with time. This time region, where the polymer solution exhibited light yellow color, coincides with region 1 of the SANS experiment. On the other hand, M_n did not effectively change from 8 to 11 h after polymerization, as shown in the central lightly shaded area in Figure 3. During this period the color of the solution gradually changed from light yellow to red. Comparing the two experiments, it is clear that this time period corresponds to region 2 in the SANS experiment, although the time interval in region 2 is quantitatively different between the two experiments, probably due to a slight difference in experimental conditions between the two. Nearly constant M_n in this time region agrees with the nearly constant q_m value in region 2. After 11 h, M_n began to increase again as shown by the right darkly shaded area in Figure 3, and the color of the solution had already changed into red in the beginning of this time region. This corresponds to region 3 in the SANS experiment.

Let us now consider the details in region 2 together with these data. For this purpose it is crucial for us to recognize that there are two regions (regions 2 and 3) which have distinctly different behaviors in the time evolution of microscopic parameters such as M_n and q_m as well as macroscopic parameter regarding the solution color, which reflects back the microscopic state of the living chain end, as highlighted and summarized in Table 2. To visualize the reaction in region 2 in contrast to that in region 3, we may think of the following two possible scenarios at least. Unfortunately, we could not evaluate monomer conversion as a function of time in this preliminary experiments, partly because we could not extract polymer solutions at a given time during the SANS experiments of the polymerization process for the GPC analysis of monomer conversion and partly because UV−vis absorption spectra for isoprene and styrene monomers are significantly overlapping with those for benzene. The extraction of highly viscous solutions from the reaction cell without killing the living ends in the cells needs special cares.

Scenario 1. Before commencement of region 2, the monomers I are completely consumed, and S very slowly react with PILi until all or almost all PILi's are converted to PSLi. The slower reaction rate of PILi to S in region 2 than the reaction rate of PILi to I in region 1, as evidenced by Figure 3, can be understood by the copolymerization kinetics given by eq 1, $k_{II} > k_{IS}$. The characteristic features of region 2 as highlighted by Table 2 may be best interpreted on the basis of the following hypotheses: (i) The chain-end association structure of PILi developed in region 1 is maintained in region 2 until all or most of PILi's are converted to PSLi's, and (ii) the association structure controls reactivity of PSLi and S such that $k_{SS} \cong k_{IS}$ in region 2 ("PILi-association-induced slowing down of k_{SS}") rather than normal $k_{SS} > k_{IS}$. The reaction rates for PSLi to S are very low in region 2 so that the increase of DP or M_n is very small, which explains almost constant M_n and q_m in this region. When all chain ends are converted to PSLi, the structure of chain-end association may be changed so that $k_{SS} > k_{II}$ or k_{IS} as given by eq 1.

Scenario 2. Before commencement of region 2, a small amount of I exists, which creates tapered sequence of I and S in region 2. Though $k_{II} > k_{IS}$ in eq 1, the reaction rate of PILi to I decreases with time, as concentration of I, [I], further decreases with time. Hence, it becomes comparable to or less than the reaction rate of PILi to S. Therefore, the slow reaction of PILi to S occurs to create PSLi. Under the condition of $k_{SI} > k_{SS}$ in eq 1 but [I] ≪ [S], the reaction rate of PSLi to I keeps decreasing with time because of decreasing [I] and is eventually outweighed by PSLi to S. The PSLi reacts with either I (to create PSILi) or S (to create PSSLi). The reaction rate of PSLi to S is also suppressed by the association-induced slowing down of k_{ss} in region 2 as postulated in scenario 1. These factors may cause slow reaction to create a tapered short block sequence of I and S in region 2.

In both scenarios a slight increase of $I(q_m)$ with t (see Figure 2 in region 2) may be a consequence of a slight increase of the length or volume fraction of the block sequence. At present both scenarios seem to be probable, though we favor scenario 2. A clear-cut distinction of the two deserves future works, for which a simultaneous measurement of monomer conversions of S and I is crucial. Strikingly enough our results elucidate that k_{SS} in region 2, $(k_{SS})_{region\ 2}$, is much smaller than k_{SS} in region 3, $(k_{SS})_{region\ 3}$,

$$(k_{SS})_{region\ 2} \ll (k_{SS})_{region\ 3} \quad (2)$$

We postulate that this is a consequence of PILi-association-induced slowing down of k_{SS}. This result given by eq 2 is commonly applied to both scenarios.

Hashimoto and co-workers have studied the anionic synthesis of tapered bcps of S and I as well as S and butadiene (B).[35−37] In both cases, THF was added as a randomizer in the reaction system comprised of the two kinds of the monomers with *sec*-BuLi in benzene. The initiation and propagation of S or B polymerization with *sec*-BuLi were dramatically accelerated by adding a small amount of THF, as reported first by Dolgoplosk.[38] These results also suggest that the chain-end aggregation control the reactivity of two monomers. In the Appendix we shall present our preliminary experimental results showing that an addition of a small amount of THF into the present reaction system accelerates the polymerization rate and made clear distinction from region 1 to 3 invisible.

C. Region 3. In region 3, $I(q_m)$ and q_m rapidly increased and decreased with time, respectively. After all PILi had changed into PI−S−Li in the end of region 2, PI−S−Li rapidly reacted with S, resulting in producing PI-*block*-dPS which probably contains a short tapered sequence of S and I in between PI and PS blocks in the case when scenario 2 is applied to region 2. At $t > 32\,107$ s, a discontinuous change in the width of the peak at q_m was first observed as shown in Figure 1b, and then appearance of the higher-order peaks at $\sqrt{3}$ and $\sqrt{7}$ positions of q_m was observed, indicating that order−disorder transition (ODT) occurred and then the hexagonally packed cylindrical microdomains of dPS are formed in the matrix of PI.

The discontinuous change in the peak width is more clearly seen in Figure 4 where square of the half-width at half-maximum value, σ_q^2, is plotted as a function of the reaction time. In our experimental conditions, the scattering contrast is obtained only between PI and the other components, so that the microdomain structure of PI-*block*-dPS can be observed by SANS. Although there have been many studies on ODT of bcps, the ODT observed in this study is not induced by temperature[39−44] or pressure changes[45,46] as reported by the previous works, but rather by the changes in the degree of polymerization and polymer concentration in the solution. Therefore, this may be the first report on the polymerization-induced ODT.

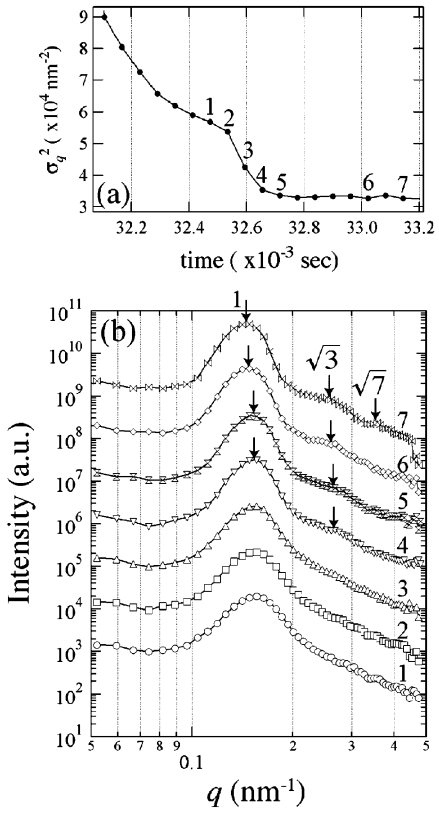

Figure 4. (a) σ_q^2 (square of the half-width at half-maximum of the first-order peak) plotted as a function of time. (b) Time change in the scattering profile at particular time labeled 1−7 in (a). The profiles are shifted vertically by 1 decade for clarity.

It should be noted that the discontinuity is "seemingly" accompanied by the structural change from the disordered structure with thermal concentration fluctuations (profiles 1 and 2) to hexagonal cylinders (profiles 4 and 5) as may be evidenced by the change in the scattering profiles shown in Figure 4b. The assertion of profiles 4 and 5 reflecting hexagonal cylinder is based upon the fact that these profiles have the value of σ_q^2 equal to that for the profiles obtained after 33.0×10^3 s (profile 7), which clearly exhibits the third-order peak at $\sqrt{7}q_m$, typical of hexagonal cylinders. If this is the case, the set of our scattering data does not show up clearly the existence of body-centered-cubic (bcc) spheres comprised of PSLi block chains with increasing the reaction time or volume fraction, f_{dPS}, and DP of dPSLi block chains.

The intriguing observation as described above reflects either one of the following three cases: (i) A time span for bcc spheres exists is very short (in between the time which gives profile 2 (32 534 s) and that which give profile 4 (32 655 s) in Figure 4. (ii) Ordering of spheres occurs at much slower rate than the polymerization rate of PS block and ordering rate of cylinders. (iii) Ionic interactions at living chain ends destabilize the bcc spheres and stabilize the hexagonal cylinders. We think the case (iii) is feasible from the viewpoint that ionic association of PS chain ends inside the minority microphase may alter conformational entropy and translational entropy of PS block chains. If the large aggregates are worm-like micelles comprised of multiple ion-pairs,[18] the existence would suppress formation of spherical microdomains and enhance that of cylindrical microdomains. This possibility should be tested by comparing morphology, as observed in-situ by SANS, for the system at specific times of the living polymerization process with that for the same system terminated at the same specific times. This experiment deserves future works. It may be worth noting that there are some related papers concerning effects of ionically end-functionalized bcps on phase behavior, phase transition, and morphology.[47−50] If (iii) is the case, this is quite unique in polymerization-induced ODT because the discontinuity or the ODT brought by the increase of f_{dPS} and DP of dPSLi is usually accompanied by the structural change from the disordered structure (spherical micelles having liquidlike spatial arrangement (the so-called disordered spheres[51])) to the bcc spheres. The ODT is a consequence of increase of χN and of increase of f_{dPS} from 0 to $^1/_2$ with time, the time changes of which also involve an increase of bcp concentration. The hexagonal cylinder was found to exist between $t \cong 32\,700$ and 39 000 s.

After $t \geq 41\,500$ s, the higher-order peaks at the integer-multiple positions (2 and 3) of q_m was observed in Figure 1b, indicating that the polymerization-induced order−order transition (OOT) occurred from the hexagonally packed cylinders to the lamellar microdomains. After $t = 46\,000-66\,000$ s the profile showed almost no change with time, as also revealed in Figure 2.

Although the time-resolved SANS measurement during bcp polymerization introduced in this paper is nothing but an initial study, we could demonstrate that this technique could be applied to the structural analysis of many different systems during chemical reactions and would contribute to understanding of the reactions from the viewpoint of structural changes. Moreover, since we can clearly observe the change of microdomain morphology during polymerization, it is possible to freeze the system and to obtain the desirable microdomain structure whenever necessary. For this purpose also it is crucial to clarify whether or how significantly the ionic association of chain ends affects the morphology.

V. Concluding Remarks

In-situ and time-resolved observation of the self-assembling process is one of the essential works for future development of nanotechnology. In this study, we carried out the in-situ observation of the molecular self-assembly induced by living anionic polymerization process of polyisoprene-*block*-poly(styrene-d_8) (PI-*block*-dPS) in benzene-d_6 as a solvent by means of the time-resolved SANS measurement. Polymerization was started in a condition of S and I coexisting in the system at a high concentration without stirring, and the difference of reactivity between two monomers produced the bcp.

The schematic illustration of the polymerization process in this study is shown in Figure 5 where counterions, Li^+, were ignored for the sake of simplicity. By the time-resolved SANS measurement, we confirmed three different time regions (regions 1−3) in this polymerization process. In region 1, the living polymer solution had a light yellow color, suggesting the presence of PILi (part a). Therefore, region 1 is the period that the PILi selectively reacts with I, and then PILi propagate as schematically shown by black lines. Besides, the scattered intensity in the low-q region at $q < 0.1$ nm^{-1} increased with time (Figure 1), indicating that PILi chains associate and form "aggregates" in region 1 (Figure 5a). The aggregates in region 1 have such a special characteristic that the living anions allows to selectively react with I but not with S, giving rise to $k_{SI} > k_{SS}$, and $k_{II} > k_{IS}$ shown in eq 1. The selective monomer consumption was elucidated also by a simultaneous observation of SANS and GPC focused on I and S concentrations during the reaction on a separate experiment.[39] We shall not touch on further detailed discussion about nature of the aggregates. However, the low-q upturn observed in the experiments is considered to arise from miceller aggregates of multiple ion pairs as proposed by Stellbrink et al.[18]

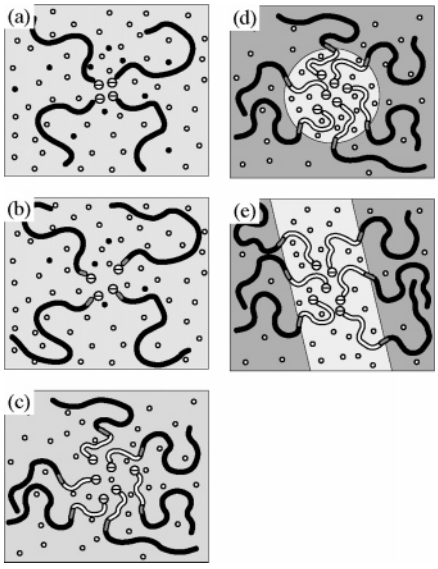

Figure 5. Schematic illustrations of polymerization process in this study (filled circles: isoprene monomer; unfilled circles: styrene-d_8 monomer; black chains: PI; white chains: dPS; short gray parts between black and white chians: tapered sequence or a short S sequence): (a) representation of region 1, (b) region 2, (c−e) region 3, where the changes from (c) to (d) and from (d) to (e) demonstrate respectively ODT and OOT.

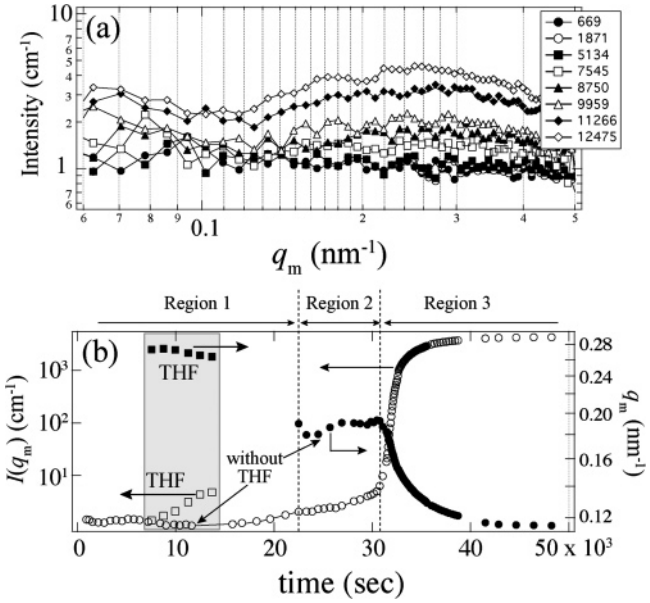

Figure 6. (a) Time evolution of SANS profiles during the living anionic polymerization of the system containing a small amount of THF. The numbers in the legend indicate the time in unit of seconds after onset of polymerization reaction. (b) The time evolution of the maximum intensity $I(q_m)$ and the magnitude of the scattering vector q_m at the maximum intensity. The data for the reaction system with THF, which exists in the shaded zone, are labeled by the word "THF" and are plotted on the common scale with the data for the system without THF, which are deliberately included for reference.

In region 2, most or all of I were consumed, and only a few S may react very slowly with PILi. In this region, a peak appeared at $q = q_m \cong 0.2$ nm^{-1}, and the intensity slightly increased with time (Figure 1), while the peak position q_m and molecular weight remained almost constant (Figures 2 and 3 and Table 2), suggesting that some of the PILi reacted with S and changed into PI−S−Li. However, the chain propagation of PI−SLi occurs extremely slowly until almost all PILi change into PSLi (association-induced suppression of k_{SS} discussed in section IV.B), judging from the solution color and molecular weight analysis shown in Figure 3. Therefore, in region 2 a short PS block sequence or tapered block sequence poly(I/S)$^-$ may be formed, as schematically shown in Figure 5b by the gray part of chains. This behavior was probably caused by the presence of the aggregates in region 2 which have almost the same characteristic as those in region 1. The small increase of the peak intensity $I(q_m)$ may be a consequence of a small increase of volume fraction of the block sequence toward $^1/_2$. Almost no change of q_m in region 2 may be a consequence of the block sequence formed being kept very short.

In region 3, the peak position rapidly shifted toward smaller q, and its intensity also rapidly increased, suggesting a rapid growth of PS block chains (the bright chains) attached to the short block chains (gray lines) as shown in Figure 5c. The living chain ends of PI-*block*-PSLi are expected to form ion aggregates which are much more reactive to S than PILi: An alteration of the chain ends poly(I/S)$^-$ to styryllithium (in scenario 2 in region 2) may drastically change the nature of the ion aggregates and strongly enhance reactivity with S. In this time region, the order−disorder transition (ODT) from the disorder state to the cylindrical microdomain structure (Figure 5c,d) and order−order transition (OOT) from cylindrical to lamellar structure occurred (Figure 5d,e).

In the time-resolved SANS measurement, we could observe the dramatic changes in the reaction-induced self-assembly between region 1 (propagation of PILi) and region 3 (propagation of PI-*block*-dPSLi) through the transition region designated region 2. Especially, in region 2, we could elucidate the unique behavior that the aggregates of PILi control the reactivity of S monomers with PSLi as given by eq 2. These results suggest that we should deal with chemical reactions not only at a local scale (concerning the chemically active site in the primary structure) but also at a larger length scale (concerning aggregates of the active sites or self-assembled structures).

Acknowledgment. This work was supported in part by a Grant-in-Aid for Scientific Research (under Grant 14350497-(B)) from Japan Society for the Promotion of Science and in part by 21st century COE program, COE for a United Approach to New Materials Science. The authors gratefully acknowledge Prof. Axel Müller for his comments and discussion on this work.

Appendix

We shall present effects of adding a small amount of THF on time evolution of q_m and $I(q_m)$ to the present reaction system comprised of isoprene (I), styrene-d_8 (S), and benzene-d_6 with weight ratio of the respective components being 1:1:2. After the same simultaneous polymerization of I and S with *sec*-BuLi as an initiator as described in the text, we obtained polymers having almost identical heterogeneity index (of $M_w/M_n = 1.03$) to the polymer obtained without THF. The polymer had M_n ($= 8.08 \times 10^4$) which is slightly smaller than the polymers obtained without THF. This is due to a slightly larger effective concentration of the initiator. The results indicates that the polymerization with a small amount of THF proceeds well as in the case without THF.

Figure 6a shows the time evolution of SANS profiles measured during the living anionic polymerization in the system with THF, while the data in the gray part in Figure 6b shows the time evolution of the characteristic scattering parameters q_m and $I(q_m)$. The data are plotted on the same scale as that used for time evolution of q_m and $I(q_m)$ for the case without THF. The data for the case without THF are deliberately added

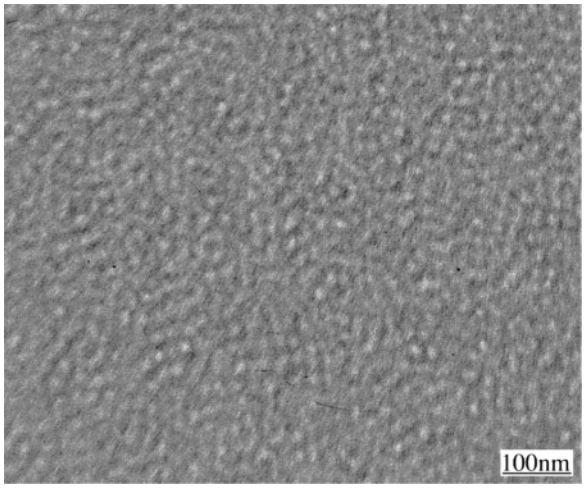

Figure 7. A typical transmission electron micrograph obtained for the ultrathin sections of the as-cast films stained with OsO_4. The polymer was synthesized via the simultaneous living anionic polymerization of styrene-d_8 and isoprene in benzene-d_6 with a small amount of THF.

for reference, though they are identical to those shown in Figure 2.

We can find the following striking differences between the two cases: (i) The scattering profiles in Figure 6a showed only a broad scattering maximum compared with those in Figure 1a, indicating enhanced intermixing of I and S units and no clear microphase-separated structure with long range order. (ii) The upturn of the SANS intensity with lowering q in the small q range can be hardly discerned in Figure 6a, implying absence of large aggregates formed by the living chain ends. (iii) The values q_m's are much larger and much less time-dependent than those for the case without THF, suggesting a complicated sequence distribution of I and S units being formed to give rise to a tapered bcp. (iv) The values $I(q_m)$'s are much smaller and much less time-dependent than those for the case without THF, which may be closely related to the difference (iii). (v) The time changes in q_m and $I(q_m)$ occur much more rapidly than those for the case without THF, implying the chain end is more free from the associations.

The striking differences as highlighted above may reflect change of the association structure of the living chain ends induced by adding a small amount of THF. The THF may weaken ionic association of living chain ends because it may increase dielectric constant of the local environment for the living chain ends, which appears to strongly alter the simultaneous living anionic polymerization process also, as clearly evidenced by the striking differences as described above. Thus, the block copolymer formed in the solution with THF is not such a diblock copolymer of PI-*b*-PS as synthesized without THF but rather a tapered bcp whose sequence distributions of S and I monomers give a broad scattering maximum and the low maximum intensity in disordered state.

The block copolymer films obtained after solvent evaporation never gave rise to well-defined ordered structure, which is highlighted by Figure 7. Figure 7 shows a typical transmission electron micrograph obtained for the ultrathin sections of the as-cast film stained with OsO_4. The image reflects a snapshot or frozen dynamical structure originating from thermal composition fluctuations in disordered state which is denoted as the D_F structure.[52−54] The frozen D_F structure shows existence of styrene-rich regions and isoprene-rich regions which are spatially arranged with a liquidlike order.

We postulate the following scenario for the effect of adding a small amount of THF on chemical reaction and reaction-induced self-assembly. THF altered local structure on ionic association of living chain ends. This effect alters the simultaneous living anionic polymerization reaction mechanism and reaction kinetics, which in turn alters reaction-induced self-assembly. The broad scattering maximum and the D_F structure may suggest that the tapered bcp formed is assumed to be a bcp comprised of a sequence rich in I and that rich in S as a rough approximation. It is needless to say a further study is required as to simultaneous observations of monomer conversions, molecular weight determination, and SANS.

References and Notes

(1) Fink, Y.; Urbas, A. M.; Bawendi, M. G.; Joannopoulos, J. D.; Thomas, E. L. *J. Lightwave Technol.* **1999**, *17*, 1963.
(2) Mansky, P.; Chaikin, P.; Thomas, E. L. *J. Mater. Sci.* **1995**, *30*, 1987.
(3) Park, M.; Harrison, C.; Chaikin, P. M.; Register, R. A.; Adamson, D. H. *Science* **1997**, *276*, 1401.
(4) Cheng, J. Y.; Ross, C. A.; Chen, V. Z. H.; Thomas, E. L.; Lammertink, R. G. H.; Vancso, G. J. *Adv. Mater.* **2001**, *13*, 1174.
(5) Naito, K.; Hieda, H.; Sakurai, M.; Kamata, Y.; Asakawa, K. *IEEE Trans. Magn.* **2002**, *38*, 1949.
(6) Leibler, L. *Macromolecules* **1980**, *13*, 1602.
(7) Hashimoto, T.; Tsukahara, Y.; Kawai, H. *J. Polym. Sci., Polym. Lett. Ed.* **1980**, *18*, 585; *Macromolecules* **1981**, *14*, 708.
(8) Roe, R. J.; Fishkis, M.; Chang, J. C. *Macromolecules* **1981**, *14*, 1091.
(9) Hashimoto, T.; Shibayama, M.; Kawai, H. *Macromolecules* **1983**, *16*, 1093.
(10) Zin, W. C.; Roe, R. J. *Macromolecules* **1984**, *17*, 183.
(11) Mori, K.; Hasegawa, H.; Hashimoto, T. *Polym. J.* **1985**, *17*, 799.
(12) Bates, F. S.; Hartney, M. A. *Macromolecules* **1985**, *18*, 2478.
(13) Hashimoto, T.; Hasegawa, H.; Hashimoto, T.; Katayama, H.; Kamigaito, M.; Sawamoto, M.; Imai, M. *Macromolecules* **1997**, *30*, 6819.
(14) Yamauchi, K.; Hasegawa, H.; Hashimoto, T.; Nagao, M. *J. Appl. Crystallogr.* **2003**, *36*, 708.
(15) Boué, F.; Lindner, P. *Europhys. Lett.* **1994**, *25*, 421.
(16) Saito, S.; Koizumi, S.; Matsuzaka, K.; Suehiro, S.; Hashimoto, T. *Macromolecules* **2000**, *33*, 2153-2162.
(17) Fetters, L. J.; Balsara, N. P.; Huang, J. S.; Jeon, H. S.; Almdal, K.; Lin, M. Y. *Macromolecules* **1995**, *28*, 4996.
(18) Stellbrink, J.; Willner, L.; Jucknischke, O.; Richter, D.; Lindner, P.; Fetters, L. J.; Huang, J. S. *Macromolecules* **1998**, *31*, 4189.
(19) Stellbrink, J.; Allgaier, J.; Willner, L.; Richter, D.; Slawecki, T.; Fetters, L. J. *Polymer* **2002**, *43*, 7101.
(20) Niu, A. Z.; Stellbrink, J.; Allgaier, J.; Willner, L.; Radulescu, A.; Richter, D.; Koenig, B. W.; May, R. P.; Fetters, L. J. J. *J. Chem. Phys.* **2005**, *122*, 134906.
(21) It should be noted that the evaluation of the association number[17−20] according to the method as described in the text needs special care for such systems as ours which involve overlaps of chains.
(22) Watanabe, H.; Oishi, Y.; Kanaya, T.; Kaji, H.; Horii, F. *Macromolecules* **2003**, *36*, 220.
(23) Motokawa, R.; Nakahira, T.; Annaka, M.; Hashimoto, T.; Koizumi, S. *Polymer* **2004**, *45*, 9019.
(24) Shibayama, M.; Ikkkai, F.; Nomura, S. *Macromolecules* **1994**, *27*, 6383.
(25) Sugihara, S.; Hashimoto, K.; Okabe, S.; Shibayama, M.; Kanaoka, S.; Aoshima, S. *Macromolecules* **2004**, *37*, 336.
(26) Motokawa, R.; Koizumi, S.; Annaka, M.; Nakahira, T.; Hashimoto, T. *Prog. Colloid Polym. Sci.* **2005**, *130*, 85.
(27) Worsfold, D. J. *J. Polym. Sci., Part A* **1967**, *5*, 2783.
(28) de Gennes, P. G. *Scaling Concepts in Polymer Physics*; Cornell University Press: Ithaca, NY, 1979.
(29) Worsfold, D. J.; Bywater, S. *Can. J. Chem.* **1964**, *42*, 2884.
(30) Medvedev, S. S. *Dokl. Nat. Acc. Nauk SSSR* **1962**, *146*, 368.
(31) Sinn, H.; Patat, F. *Angew. Chem.* **1963**, *75*, 805.
(32) Johnson, A. F.; Worsfold, D. J. *J. Polym. Sci.* **1961**, *A3*, 444.
(33) Worsfold, D. J.; Bywater, S. *ACS Polym. Prepr.* **1986**, *27*, 140.
(34) We assume overlap concentration is attained during polymerization of isoprene. $c^*(t)$ in volume fraction of PI is given by $c^*(t) = N(t)a^3[(4\pi/3)R_g(t)^3]^{-1}$, where a and R_g are the segment length and radius of gyration, respectively. Assuming unperturbed chain dimension of PI for a rough estimation of $c^*(t)$, $R_g(t)$ is given by $R_g(t)^2 = (1/6)N(t)\,a^2$. Now $c(t)$ is given by $c(t) = n_pN(t)\,a^3$, where $n_p = c_m/N_{PI}$ and c_m is number of isoprene monomers per unit volume. By setting $c^*(t^*) = c(t^*)$ at $t = t^*$, $N_{PI} = 735$ from Figure 3, $a = 0.658$ nm, and

$c_m = 1.89\ nm^{-3}$, we can estimate $N(t^*) = 280$ and hence $M(t^*) = 1.9 \times 10^4$. This value of $M(t^*)$ together with the data in Figure 3 yields $t^* \cong 4 \times 10^3$ s.
(35) Tsukahara, Y.; Nakamura, N.; Hashimoto, T.; Kawai, H.; Nagaya, T.; Sugimura, Y.; Tsuge, S. *Polym. J.* **1980**, *12*, 455.
(36) Hashimoto, T.; Tsukahara, Y.; Kawai, H. *Polym. J.* **1983**, *15*, 699.
(37) Hashimoto, T.; Tsukahara, Y.; Tachi, K.; Kawai, H. *Macromolecules* **1983**, *16*, 648.
(38) Kropacheva, E. N.; Dolgoplosk, B. A.; Kuznetsova, E. M. *Dokl. Akad. Nauk SSSR* **1960**, *130*, 1253.
(39) Tanaka, H.; Yamauchi, K.; Hasegawa, H.; Miyamoto, N.; Koizumi, S.; Hashimoto, T. Manuscript in preparation.
(40) Bates, F. S.; Rosedale, J. H.; Fredrickson, G. H. *J. Chem. Phys.* **1990**, *92*, 6255.
(41) Wolff, T.; Burger, C.; Ruland, W. *Macromolecules* **1993**, *26*, 1707.
(42) Stühn, B.; Mutter, R.; Albrecht, T. *Europhys. Lett.* **1992**, *18*, 427.
(43) Ogawa, T.; Sakamoto, N.; Hashimoto, T.; Han, C. D.; Baek, D. M. *Macromolecules* **1996**, *29*, 2113.
(44) Koga, T.; Koga, T.; Hashimoto, T. *J. Chem. Phys.* **1999**, *110*, 11076.
(45) Schwahn, D.; Frielinghaus, H.; Mortensen, K.; Almdal, K. *Phys. Rev. Lett.* **1996**, *77*, 3153.
(46) Migler, K. B. M.; Han, C. *Macromolecules* **1998**, *31*, 360.
(47) Bartels, V. T.; Stamm, M.; Mortensen, K. *Polym. Bull. (Berlin)* **1996**, *36*, 103.
(48) Schädler, V.; Kniese, V.; Thurn-Albrecht, T.; Wiesner, U.; Spiess, H. W. *Macromolecules* **1998**, *31*, 4828.
(49) Schöps, M.; Leist, H.; DuChesne, A.; Wiesner, U. *Macromolecules* **1999**, *32*, 2806.
(50) Choi, S.; Han, C. D. *Macromolecules* **2003**, *36*, 6220.
(51) Han, C. D.; Vadiya, N. Y.; Kim, D.; Shin, G.; Yamaguchi, D.; Hashimoto, T. *Macromolecules* **2000**, *33*, 3767.
(52) Sakamoto, N.; Hashimoto, T. *Macromolecules* **1998**, *31*, 3815.
(53) Hashimoto, T.; Koga, T.; Koga, T.; Sakamoto, N. In *The Physics of Complex Liquids*; Yonezawa, F., Tsuji, K., Kaji, K., Doi, M., Fujiwara, T., Eds.; World Scientific: Singapore, 1999; pp 291−308.
(54) Hashimoto, T. *Macromol. Symp.* **2001**, *174*, 69.

MA052696S